Accepted Manuscript

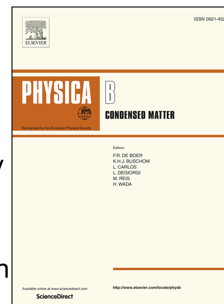

Effect of strains on electronic and optical properties of monolayer SnS: Ab-initio study

Doan Q. Khoa, Chuong V. Nguyen, Huynh V. Phuc, Victor V. Ilyasov, Tuan V. Vu, Nguyen Q. Cuong, Bui D. Hoi, Dung V. Lu, E. Feddi, M. El-Yadri, M. Farkous, Nguyen N. Hieu

PII: S0921-4526(18)30424-1

DOI: 10.1016/j.physb.2018.06.024

Reference: PHYSB 310932

To appear in: *Physica B: Physics of Condensed Matter*

Received Date: 29 May 2018

Revised Date: 19 June 2018

Accepted Date: 21 June 2018

Please cite this article as: D.Q. Khoa, C.V. Nguyen, H.V. Phuc, V.V. Ilyasov, T.V. Vu, N.Q. Cuong, B.D. Hoi, D.V. Lu, E. Feddi, M. El-Yadri, M. Farkous, N.N. Hieu, Effect of strains on electronic and optical properties of monolayer SnS: Ab-initio study, *Physica B: Physics of Condensed Matter* (2018), doi: 10.1016/j.physb.2018.06.024.

This is a PDF file of an unedited manuscript that has been accepted for publication. As a service to our customers we are providing this early version of the manuscript. The manuscript will undergo copyediting, typesetting, and review of the resulting proof before it is published in its final form. Please note that during the production process errors may be discovered which could affect the content, and all legal disclaimers that apply to the journal pertain.

ACCEPTED MANUSCRIPT

Effect of strains on electronic and optical properties of monolayer SnS: Ab-initio study

Doan Q. Khoa [a,b], Chuong V. Nguyen [c,*], Huynh V. Phuc [d], Victor .V. Ilyasov [e], Tuan V. Vu [a,b], Nguyen Q. Cuong [f], Bui D. Hoi [f], Dung V. Lu [g], E. Feddi [h], M. El-Yadri [h], M. Farkous [h], Nguyen N. Hieu [i,*]

[a]*Division of Computational Physics, Institute for Computational Science, Ton Duc Thang University, Ho Chi Minh City, Viet Nam*

[b]*Faculty of Electrical and Electronics Engineering, Ton Duc Thang University, Ho Chi Minh City, Viet Nam*

[c]*Department of Materials Science and Engineering, Le Quy Don Technical University, Ha Noi, Viet Nam*

[d]*Division of Theoretical Physics, Dong Thap University, Dong Thap 870000, Viet Nam*

[e]*Department of Physics, Don State Technical University, Rostov on Don 344000, Russia*

[f]*Department of Physics, University of Education, Hue University, Hue, Viet Nam*

[g]*Department of Physics, University of Education, The University of Da Nang, Da Nang, Viet Nam*

[h]*LaMCScI, Group of Optoelectronic of Semiconductors and Nanomaterials, ENSET, Rabat, Mohammed V University in Rabat, Rabat, Morocco*

[i]*Institute of Research and Development, Duy Tan University, Da Nang 550000, Viet Nam*

Abstract

Preprint submitted to Elsevier *22 June 2018*

ACCEPTED MANUSCRIPT

ACCEPTED MANUSCRIPT

In this work, we consider the effect of biaxial ε_b and uniaxial $\varepsilon_{ac/zz}$ strains on electronic properties and optical parameters of monolayer SnS using first-principles calculations. Our calculations show that the monolayer SnS is a semiconductor with an indirect energy gap of 1.63 eV at the equilibrium state. While an effect of tensile strains on bandgap is quite small, the bandgap of monolayer SnS depends strongly on the compressive strains, especially a semiconductor-metal phase transition is occurred due to the uniform compressive biaxial strain at -14% elongation. The optical spectra of the monolayer are high anisotropic, and the absorption coefficient of monolayer SnS tends to increase in the presence of compression strains, while the tensile strains reduce the absorption coefficient of the monolayer SnS. We believe that the phase transition and extraordinary optical properties of the strained monolayer SnS will make it become a useful material in nanoelectromechanical devices and optoelectronic applications.

Key words: Monolayer SnS, strain, band structure, optical properties, firs-principles

1 Introduction

Graphene has been the most interesting two-dimensional (2D) material for almost last two decades, both theoretical and experimental studies [1–3]. However, as a semiconductor with zero bandgap, graphene is considered as an obstacle in electronic technologies. In parallel with the research on 2D graphene, such as controlling bandgap by strain, external electric field, or placed on substrates and graphene-based heterostructures [4–10], one searched for new materials that could overcome the limitations of graphene. Phosphorene and transition metal dichalco-

* Corresponding authors.
Email addresses: doanquockhoa@tdt.edu.vn (Doan Q. Khoa), chuongnguyen@gmail.com (Chuong V. Nguyen), hieunn@duytan.edu.vn (Nguyen N. Hieu).

genide monolayers are very promising candidates which recently join the 2D family [11–14]. Due to their original optical and magneto-optical properties ranging in the visible, the dichalcogenides are expected to have many applications in optoelectronic and spintronic devices [12, 15]. However, the limitation of transition metal dichalcogenide materials is low carrier mobility which is not good for applications in optoelectronic devices [16]. Recently, 2D monochalcogenides are increasingly being studied because they have many outstanding physical properties, such as large natural bandgap, high carrier mobility and optical absorption, and good structural stability [17–20]. In parallel with theoretical predictions [21, 22], success in experimental synthesis [23–25] has opened a promising future for the 2D monochalcogenides. In contrast to gapless graphene, the monolayer monochalcogenides with large bandgap and high optical absorption are very suitable for applications in nanoelectromechanical systems and optoelectronic devices [26–28].

Because chalcogenide atom in the compound is S, SnS is predicted to be the large bandgap semiconductor compared to other monochalcogenides such as SnSe or SnTe [22]. The structural properties and stability of group IV compounds, including monolayer SnS, have been investigated by first-principles study [29]. The electronic properties and optical parameters of monolayer SnS have been calculated by several groups [30–32]. The in-plane elastic stiffness of monolayer SnS is quite hight, up to 26.02 N/m [22]. Also, Zhang and co-workers showed that monolayer SnS has a negative Poisson's ratio similar to the phosphorene [33], which is still stable under strain up to 27% [34]. Based on the calculations of phonon spectra, Singh and coworkers showed that the monolayer SnS is dynamically stable [31]. Besides, one indicated that the monolayer SnS is stable under strain ranged from -20% to 20% [33]. At the equilibrium state, the monolayer SnS is an indirect bandgap semiconductor with a high electron mobility of 1.93×10^3 cm^{-2}/Vs [32]. The calculated results for bandgap of monolayer SnS is strongly depended on the

selected functionals. Ma and coworkers showed that the bandgap of monolayer SnS is respectively equal to 1.61 eV and 2.26 eV by Perdew Burke-Ernzerhof (PBE) and Heyd-Scuseria-Ernzerhof 06 (HSE06) functionals [35]. Effect of mechanical strains on the electronic and optical properties of monolayer SnS has also been considered by density functional theory (DFT) calculations [22]. Based on calculations for the optical parameters, Huang and coworkers showed that the monolayer SnS has high absorption efficiency in the visible light regime [22]. This character is important for applications in solar cell technology. Recently, heterostructures based on SnS have also been investigated by the different approaches [36–38].

In this work, we theoretically investigate the electronic and optical properties of the monolayer SnS in the presence of the strain using first-principles calculations. We focus on the effect of biaxial and uniaxial strains on band structure and bandgap of the monolayer SnS. Effect of the strains on the optical parameters in the energy range from 0 to 8 eV is also investigated and discussed. Also, it should be noted that defects may be generated under biaxial strain in practice, which have a great influence on the carrier mobility of materials, especially to SnS. As we know that the curvature of conduction band minimum/valence band maximum (CBM/VBM) dominate the effective mass of hole/electron, and the variation of the effective mass will bring an obvious change to the carrier mobility of the SnS monolayer. We thus can expect that the mobility of electron/hole should reduce with an applying strain in the SnS monolayer. However, it is found that the carrier mobility of SnS monolayer may gradually decrease under rising strain, but is still large and could be used for designing high-performance nanoelectronic devices like field-effect transistors.

ACCEPTED MANUSCRIPT

ACCEPTED MANUSCRIPT

2 Theoretical model and method

In this work, our DFT calculations for structural parameters and electronic properties of the monolayer SnS (Fig. 1) were performed by using the Quantum Espresso package [39] with the generalized gradient approximations (GGA). The PBE has been used to optimize the structure of the monolayer SnS, and we used the $(15 \times 15 \times 1)$ k-mesh Monkhorst-Pack grid for sampling the first Brillouin zone. The kinetic energy cut-off for plane-wave basis was set as 500 eV, and the monolayer SnS structure is fully relaxed with force acting on each atom less than 10^{-6} eV/Å.

In this work, during considering the optical properties, we focus on the dielectric function $\varepsilon(\omega)$, the absorption coefficient $\alpha(\omega)$, and the electron energy loss spectrum $L(\omega)$ of the monolayer SnS. In order to calculate the dielectric function $\varepsilon(\omega) = \varepsilon_1(\omega)+i\varepsilon_2(\omega)$, we will calculate both real $\varepsilon_1(\omega)$ and imaginary $\varepsilon_2(\omega)$ parts. In principle, the $\varepsilon_1(\omega)$ could be calculated via the Kramers-Kronig transformation from the $\varepsilon_2(\omega)$, which can be written as follows [21,40]:

$$\begin{aligned}\varepsilon_2^{ij}(\omega) =& \frac{4\pi^2 e^2}{V m^2 \omega^2} \sum_{\mathbf{k}nn'\sigma} \langle \mathbf{k}n\sigma \left| p_i \right| \mathbf{k}n'\sigma \rangle \langle \mathbf{k}n'\sigma \left| p_j \right| \mathbf{k}n\sigma \rangle \\ & \times f_{\mathbf{k}n}(1 - f_{\mathbf{k}n'}) \delta(E_{\mathbf{k}n'} - E_{\mathbf{k}n} - \hbar\omega), \end{aligned} \quad (1)$$

where ω is the angular frequency of the electromagnetic irradiation, V stands for the unit-cell volume, e and m are respectively the charge and mass of electron, $\mathbf{p}$ is the momentum operator, $|\mathbf{k}n\sigma\rangle$ term represents the wave function of the crystal of the eigenvalue $E_{\mathbf{k}n}$ with the spin σ and the wavevector $\mathbf{k}$, and $f_{\mathbf{k}n}$ is the Fermi distribution function.

The absorption coefficient $\alpha(\omega)$ and the electron energy loss spectrum $L(\omega)$

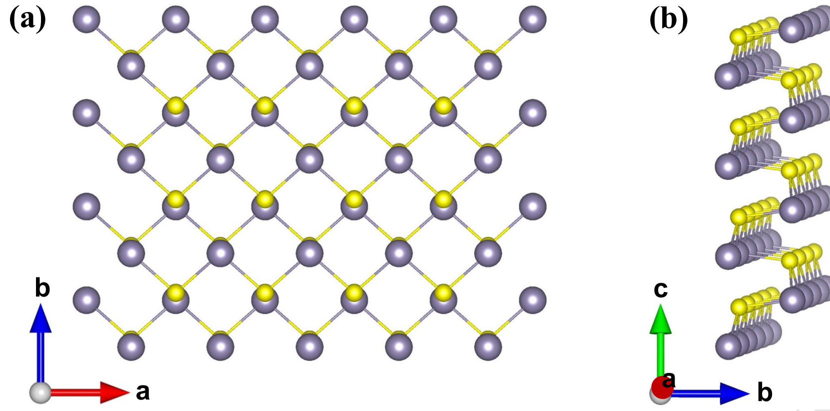

Fig. 1. (Color online) Atomic structure of the monolayer SnS: (a) top view and (b) side view. The gray and yellow balls stand respectively for the Sn and S atoms.

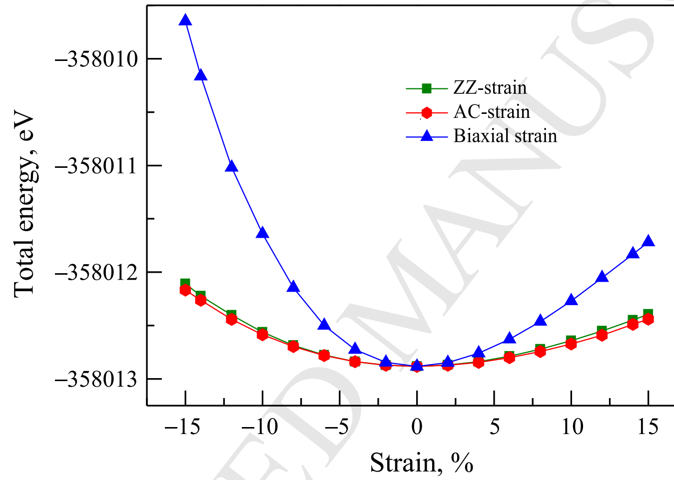

Fig. 2. (Color online) Dependence of total energy of monolayer SnS on strains.

can be calculated via the dielectric function $\varepsilon(\omega)$ as the followings [41]

$$\alpha(\omega) = \frac{\sqrt{2}\omega}{c}\left[\sqrt{\varepsilon_1^2(\omega)+\varepsilon_2^2(\omega)}-\varepsilon_1(\omega)\right]^{1/2}, \tag{2}$$

$$L(\omega) = -Im(\varepsilon^{-1}) = \frac{\varepsilon_2(\omega)}{\varepsilon_1^2(\omega)+\varepsilon_2^2(\omega)}. \tag{3}$$

3 Results and discussion

The atomic structure of monolayer SnS is shown in Fig. 1. At equilibrium, the lattice constants of the monolayer SnS are $a = 4.084$ Å and $b = 4.286$ Å. These

ACCEPTED MANUSCRIPT

parameters are very close to the result of the previous DFT calculations [22, 42]. Previous experimental work showed that the bulk SnS has an orthorhombic structure with two phases which are depending on the temperature: α-phase at low temperatures (< 873 K) and β-phase at higher temperatures [43]. A naturally occurring mineral of the bulk SnS has the orthorhombic structure which belongs to the space group $Pnma$, known as α-phase of SnS [44, 45]. Our calculations provides that the lattice parameters of the bulk structure of SnS after relaxation is $a = 4.023$ Å, $b = 4.323$ Å, and $c = 11.310$ Å. This result is in good agreement with the earlier theoretical study [46] and experimental measurements [47, 48]. In the monolayer, due to the losing translational symmetry along the z-direction and with it the inversion symmetry, the structure of Sn monolayer is in the $Pmn2_1$ space group [see also, Ref. [42]. The total energy at the equilibrium state of monolayer SnS is -358012.88 eV. From Fig. 2 we can see that the effect of uniaxial strains, i.e., applied strains along the zigzag (ZZ-strain ε_{zz}) and armchair (AC-strain ε_{ac}) directions on the total energy of the system is negligible. Meanwhile, the biaxial strain ε_b, especially compression case $\varepsilon_b < 0$, significantly affects the total energy of the monolayer SnS. Our calculations show that the monolayer SnS at equilibrium is a semiconductor with a large bandgap of 1.63 eV. This value is close to resulting in the previous DFT calculations (1.61 eV) [35]. As shown in Fig. 3(a), the lowest energy of the conduction band is on the ΓX path while the highest energy of the valence band is on the YΓ path, and so, an indirect energy gap is formed on the Fermi level. Partial density of states (PDOS) and total density of states (TDOS) of the monolayer SnS at equilibrium is shown in Fig. 3(b). We find that the TDOS is formed by the major contribution from the p-orbitals of both Sn and S. However, while the contribution of Sn-p orbital in the conduction band is dominant, the contribution of S-p orbital in the valence band is very bigger than the contribution of Sn-p orbital. Also, a significant contribution of Sn-s orbital to the valence band was

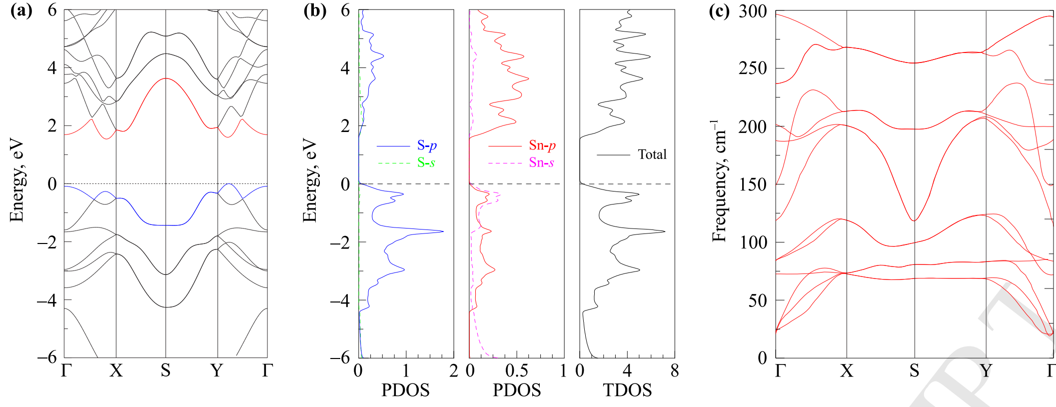

Fig. 3. (Color online) Band structure (a), density of states (b), and phonon dispersion curves (c) of monolayer SnS at equilibrium.

noted during considering the density of states of the system. To check the thermodynamic stability of the SnS monolayer, we also calculate its phonon dispersion curves, as shown in Fig. 3(c). We find that there are no soft phonon modes in the phonon spectrum of the monolayer SnS. This indicates that the monolayer SnS at the equilibrium state is dynamical stable.

In Fig. 4, we show the band structure of monolayer SnS in presence of the ZZ-strain ε_{zz}, AC-strain ε_{ac}, and biaxial strain ε_b at several elongations. From Fig. 4, we can see that the highest energy of the valence band is always close to the Fermi level ($E_F = 0$) and the strains almost only change the position of the highest energy of the valence band and do not change its value. The strains significantly effect on the conduction band of the monolayer SnS, not just the value of the lowest energy of the conduction band, but also its position, i.e., the strains can cause the position of the lowest energy of the conduction band to move from ΓX of YΓ path to Γ point. The density of states of monolayer SnS under ZZ-strain, AC-strain, and biaxial strain are also shown in Fig. 5. We found that tensile strains increased the contribution of Sn-s orbital in the density of states (DOS), especially in the valence band. From Figs. 5(c,d), we see that the peaks in the energy range from -1 to 0 have an important contribution from Sn-s orbital and the peak around -5.75 eV

ACCEPTED MANUSCRIPT

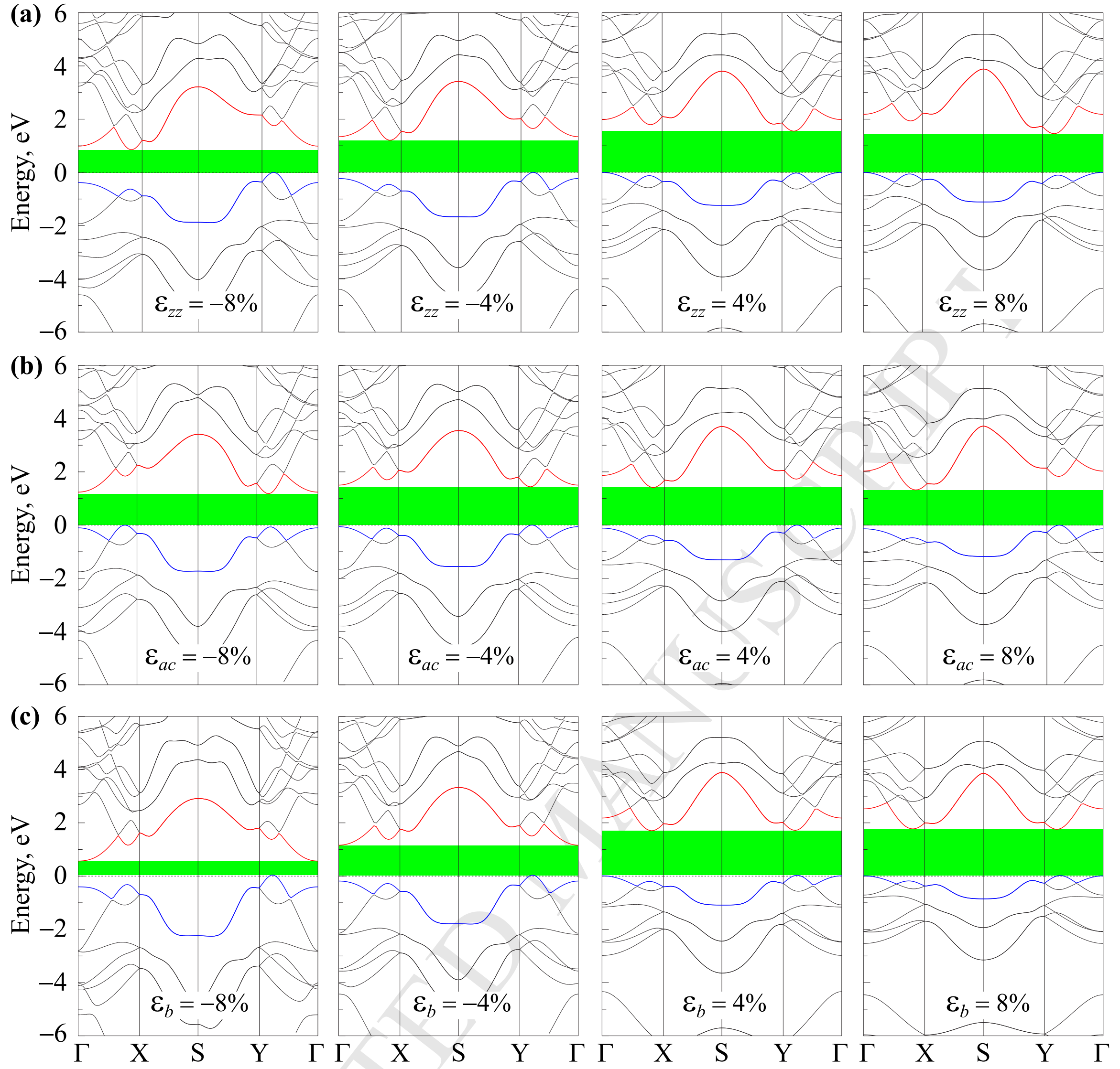

Fig. 4. (Color online) Band structure of monolayer SnS in presence of ZZ-strain ε_{zz} (a), AC-strain ε_{ac} (b), and biaxial strain ε_b (c).

formed by the main contribution from Sn-s orbital.

As analyzed above, the strains mainly change the conduction band of SnS. The effect of strains on the bandgap, as a consequence, is due to the change of the conduction band. Dependence of bandgap of monolayer SnS on the strains is shown in Fig. 6. It demonstrates that the uniaxial strains ε_{zz} and ε_{ac} almost exclusively reduces the bandgap of monolayer SnS. Besides, while the bandgap is slightly reduced by the tensile uniaxial strains ($\varepsilon_{ac/zz} > 0$), the effect of compression uniaxial

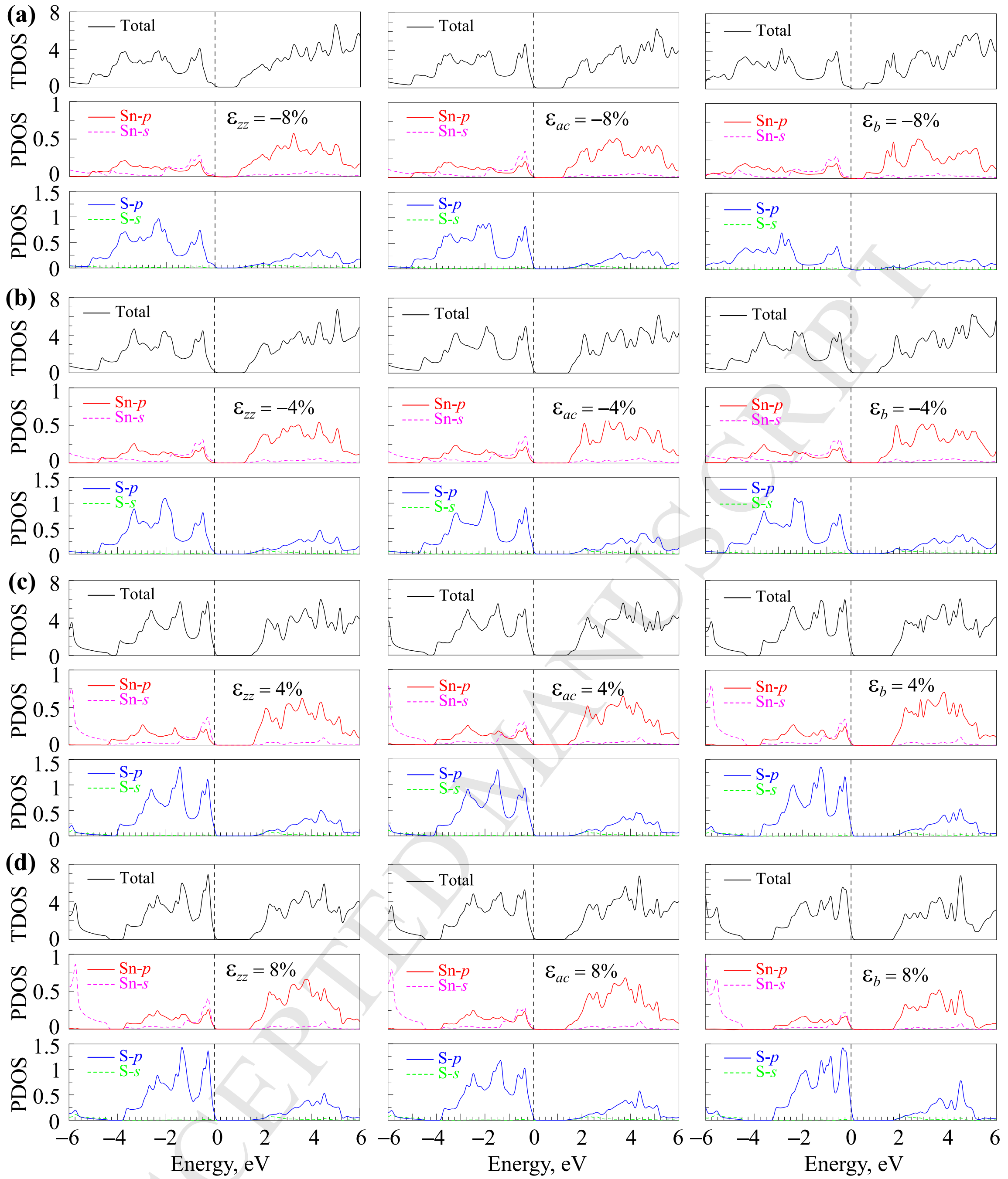

Fig. 5. (Color online) PDOS and TDOS of monolayer SnS under strains at (a) -8%, (b) -4%, (c) 4%, and (d) 8%.

strains on the bandgap of monolayer SnS was quite large. However, the excitement comes from the biaxial strain ε_b. The bandgap of monolayer SnS increased slightly and tended to remain unchanged in the presence of tensile biaxial strain ε_b. The

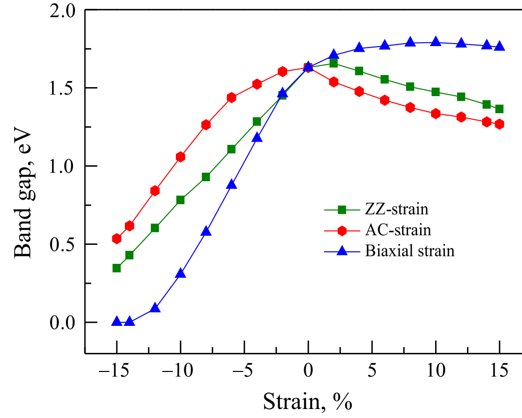

Fig. 6. (Color online) Bandgap of monolayer SnS as a function of strain.

nature of an increase in band gap value of SnS monolayer with increasing biaxial strain is relative to the position of the Fermi level. It can be seen that under biaxial strain, the VBM of the monolayer SnS is almost unchanged, whereas the conduction band minimum shifts upwards, resulting in an increase in the band gap of SnS monolayer. In contrast, under uniaxial strain the VBM/CBM of SnS monolayer shifts upwards/downwards, resulting in a decrease in its band gap. Moreover, it is well known that the SnS monolayer has an anisotropic crystal structure along both the armchair and zigzag directions. At that, there is high electric dipole moment along symmetry axis then the dipole moments along one axis can differ from each other. It indicates that the monolayer SnS shows strong anisotropic electronic properties. In contrast, the compression biaxial strain rapidly reduced the bandgap and the semiconductor-metal phase transition, i.e., bandgap equals to zero, was found at $\varepsilon_b = -14\%$. We believe that the semiconductor-metal phase transition is one of the key factors in applying the material to electro-mechanical actuators and sensors.

In next part, we briefly examine the effect of the strains on the optical characteristics of monolayer SnS. In Fig. 7, we show our calculated results of a dielectric function of monolayer SnS in the presence of both biaxial and uniaxial strains. We can see that both real part $\varepsilon_1(\omega)$ and imaginary part $\varepsilon_2(\omega)$ of the dielectric func-

ACCEPTED MANUSCRIPT

ACCEPTED MANUSCRIPT

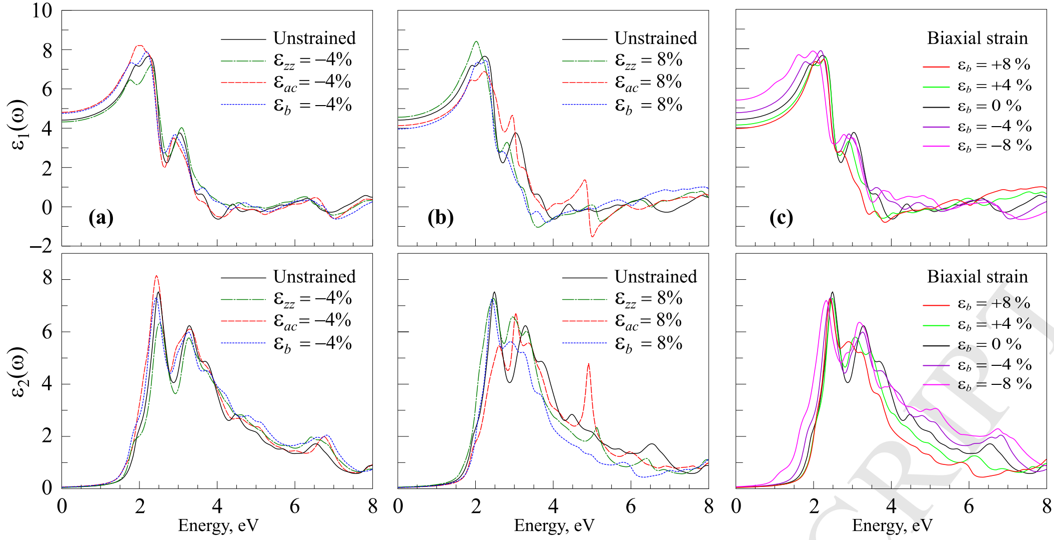

Fig. 7. (Color online) Real $\varepsilon_1(\omega)$ and imaginary $\varepsilon_2(\omega)$ parts of ε of strained monolayer SnS at elongation of -4% (a) and 8% (b). (c) Effect of biaxial strain on parts of ε of monolayer SnS at several elongations.

tion are high anisotropic. Figs. 7(a,b) show the parts of the dielectric function of monolayer SnS in the presence of biaxial and uniaxial strains at -4% and 8%, respectively. Compared with the unstrained case, we find that, when the ε is small, the shape of dielectric function spectrum of the strained SnS is similar to that of the unstrained case. However, in the case of large strain, the difference between the effect of the biaxial strain and the uniaxial strains on monolayer SnS becomes more pronounced. While biaxial strain ε_b, for example at $\varepsilon_b = 8\%$ as shown in Fig. 7(b), makes the spectrum of the dielectric function less anisotropic, the uniaxial strains make them more anisotropic, especially in the case of uniaxial strain along the armchair direction ε_{ac}. Fig. 7(c) depicts the effect of the biaxial strain ε_b on the dielectric function spectrum of the monolayer SnS.

Focusing on an absorption characters of the optical properties, we calculate the absorption coefficient of the monolayer SnS in the presence of biaxial ε_b and uniaxial $\varepsilon_{ac/zz}$ strains. It demonstrates that the absorption spectrum of the monolayer SnS is highly anisotropic, especially in the energy domain greater than 2.5eV, as

ACCEPTED MANUSCRIPT

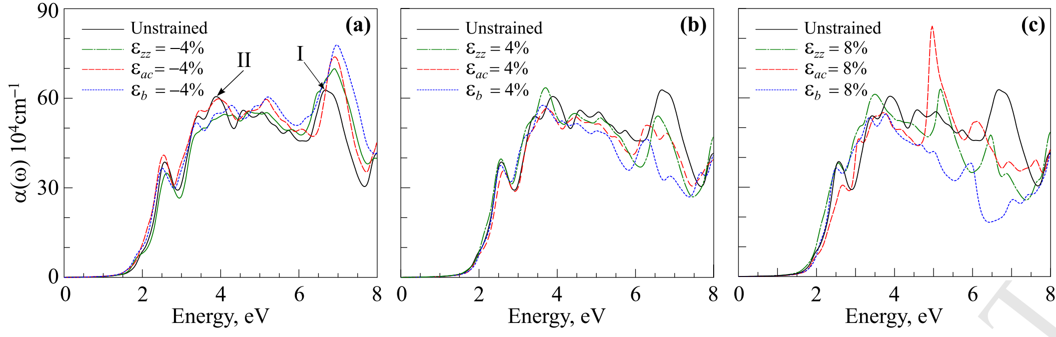

Fig. 8. (Color online) Absorption coefficient $\alpha(\omega)$ of strained monolayer SnS at elongations of -4% (a), 4% (b), and 8% (c).

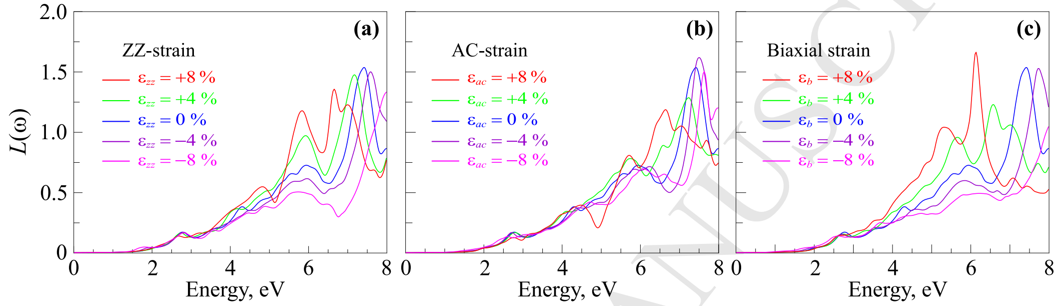

Fig. 9. (Color online) Effect of ZZ-strain ε_{zz} (a), AC-strain ε_{ac}, and biaxial strain ε_b on the electron energy loss spectrum $L(\omega)$ of monolayer SnS.

shown in Fig. 8. Our detailed calculations show that the biaxial strain ε_b reduces the absorption coefficient $\alpha(\omega)$ in tension case but increases the $\alpha(\omega)$ in the compression case. Interestingly, compared to the unstrain case, the absorption coefficient of monolayer SnS tends to increase in the presence of compression strains, while the tensile strains reduce the absorption coefficient of the monolayer SnS. At equilibrium, in the energy range from 0 to 8 eV, the maximum absorption coefficient is 62.9×10^4 cm^{-1} [peak I, Fig. 8(a)] at energy of 6.65 eV. Besides, at 3.89 eV, the absorption coefficient of monolayer SnS at equilibrium is up to 60.5×10^4 cm^{-1} (peak II). We find that the peak I is strongly increased due to the compressive strains $\varepsilon_{ac/zz}$ or ε_b while the peak II changes insignificantly. Effect of strains on the electron energy loss spectrum $L(\omega)$ is shown in Fig. 9. The effect of strains on the $L(\omega)$ is evident in the high energy domain, i.e., greater than 5 eV. The $L(\omega)$ is also

ACCEPTED MANUSCRIPT

strongly anisotropic in this energy domain.

4 Conclusion

In conclusion, we consider the electronic properties and optical parameters of the monolayer SnS in the presence of the in-plane strains ($\varepsilon_{ac}, \varepsilon_{zz}, \varepsilon_b$) is studied by DFT calculations. Our calculations show that the strain, especially the biaxial strain ε_b, strongly affects the bandgap of the monolayer SnS. The semiconductor-metal phase transition was observed at large biaxial strain of 14%. The optical spectrum of the monolayer SnS is highly anisotropic. The absorption coefficient $\alpha(\omega)$ is maximum at the energy of 6.65 eV, and this peak is significantly increased in the presence of in-plain strains.

5 Acknowledgments

This research is funded by the Vietnam National Foundation for Science and Technology Development (NAFOSTED) under Grant Number 103.01-2017.309.

References

[1] K. S. Novoselov, A. K. Geim, S. V. Morozov, D. Jiang, Y. Zhang, S. V. Dubonos, I. V. Grigorieva, A. A. Firsov, Science 306 (2004) 666.

[2] A. H. Castro Neto, F. Guinea, N. M. R. Peres, K. S. Novoselov, A. K. Geim, Rev. Mod. Phys. 81 (2009) 109.

[3] C. V. Nguyen, N. N. Hieu, C. A. Duque, N. A. Poklonski, V. V. Ilyasov, N. V. Hieu, L. Dinh, Q. K. Quang, L. V. Tung, H. V. Phuc, Opt. Mater. 69 (2017) 328.

[4] B. Verberck, B. Partoens, F. M. Peeters, B. Trauzettel, Phys. Rev. B 85 (2012) 125403.

ACCEPTED MANUSCRIPT

[5] H. V. Phuc, V. V. Ilyasov, N. N. Hieu, B. Amin, C. V. Nguyen, J. Alloys Compd. 750 (2018) 765.

[6] S. B. Kumar, J. Guo, Appl. Phys. Lett. 98 (2011) 222101.

[7] G. G. Naumis, S. Barraza-Lopez, M. Oliva-Leyva, H. Terrones, Rep. Prog. Phys. 80 (2017) 096501.

[8] H. V. Phuc, V. V. Ilyasov, N. N. Hieu, C. V. Nguyen, Vacuum 149 (2018) 231.

[9] A. K. Geim, I. V. Grigorieva, Nature 499 (2013) 419.

[10] N. N. Hieu, H. V. Phuc, V. V. Ilyasov, N. D. Chien, N. A. Poklonski, N. V. Hieu, C. V. Nguyen, J. Appl. Phys. 122 (2017) 104301.

[11] X. Li, L. Tao, Z. Chen, H. Fang, X. Li, X. Wang, J.-B. Xu, H. Zhu, Appl. Phys. Rev. 4 (2017) 021306.

[12] C. V. Nguyen, N. N. Hieu, N. A. Poklonski, V. V. Ilyasov, L. Dinh, T. C. Phong, L. V. Tung, H. V. Phuc, Phys. Rev. B 96 (2017) 125411.

[13] C. V. Nguyen, N. N. Hieu, C. A. Duque, D. Q. Khoa, N. V. Hieu, L. V. Tung, H. V. Phuc, J. Appl. Phys. 121 (2017) 045107.

[14] P. Johari, V. B. Shenoy, ACS Nano 6 (2012) 5449.

[15] C. V. Nguyen, N. N. Hieu, D. Muoi, C. A. Duque, E. Feddi, H. V. Nguyen, L. T. T. Phuong, B. D. Hoi, H. V. Phuc, J. Appl. Phys. 123 (2018) 034301.

[16] H. Wang, L. Yu, Y.-H. Lee, Y. Shi, A. Hsu, M. L. Chin, L.-J. Li, M. Dubey, J. Kong, T. Palacios, Nano Lett. 12 (2012) 4674.

[17] K. Xu, L. Yin, Y. Huang, T. A. Shifa, J. Chu, F. Wang, R. Cheng, Z. Wang, J. He, Nanoscale 8 (2016) 16802.

[18] M. Xu, T. Liang, M. Shi, H. Chen, Chem. Rev. 113 (2013) 3766.

ACCEPTED MANUSCRIPT

ACCEPTED MANUSCRIPT

[19] S. Zhang, N. Wang, S. Liu, S. Huang, W. Zhou, B. Cai, M. Xie, Q. Yang, X. Chen, H. Zeng, Nanotechnology 27 (2016) 274001.

[20] F. Li, X. Liu, Y. Wang, Y. Li, J. Mater. Chem. C 4 (2016) 2155.

[21] S. Z. Karazhanov, P. Ravindran, A. Kjekshus, H. Fjellvag, B. G. Svensson, Phys. Rev. B 75 (2007) 155104.

[22] L. Huang, F. Wu, J. Li, J. Chem. Phys. 144 (2016) 114708.

[23] S. Lei, L. Ge, Z. Liu, S. Najmaei, G. Shi, G. You, J. Lou, R. Vajtai, P. M. Ajayan, Nano Lett. 13 (2013) 2777.

[24] D. D. Vaughn, R. J. Patel, M. A. Hickner, R. E. Schaak, J. Am. Chem. Soc. 132 (2010) 15170.

[25] Y. Li, D. Wu, Z. Zhou, C. R. Cabrera, Z. Chen, J. Phys. Chem. Lett. 3 (2012) 2221.

[26] D. J. Late, L. Bin, L. Jiajun, Y. Aiming, M. H. S. S. Ramakrishna, G. Matthew, C. N. R. Rao, P. Dravid Vinayak, Adv. Mater. 24 (2012) 3549.

[27] S. Sucharitakul, N. J. Goble, U. R. Kumar, R. Sankar, Z. A. Bogorad, F.-C. Chou, Y.-T. Chen, X. P. A. Gao, Nano Lett. 15 (2015) 3815.

[28] A. M. Cook, B. M. Fregoso, F. de Juan, S. Coh, J. E. Moore, Nat. Commun. 8 (2017) 14176.

[29] M. Wu, S.-H. Wei, L. Huang, Phys. Rev. B 96 (2017) 205411.

[30] S. Demirci, N. Avazli, E. Durgun, S. Cahangirov, Phys. Rev. B 95 (2017) 115409.

[31] A. K. Singh, R. G. Hennig, Appl. Phys. Lett. 105 (2014) 042103.

[32] L. Xu, M. Yang, S. J. Wang, Y. P. Feng, Phys. Rev. B 95 (2017) 235434.

[33] Y. Zhang, B. Shang, L. Li, J. Lei, RSC Adv. 7 (2017) 30327.

[34] M. Elahi, K. Khaliji, S. M. Tabatabaei, M. Pourfath, R. Asgari, Phys. Rev. B 91 (2015) 115412.

ACCEPTED MANUSCRIPT

[35] Z. Ma, B. Wang, L. Ou, Y. Zhang, X. Zhang, Z. Zhou, Nanotechnology 27 (2016) 415203.

[36] K. Cheng, Y. Guo, N. Han, Y. Su, J. Zhang, J. Zhao, J. Mater. Chem. C 5 (2017) 3788.

[37] L. Peng, C. Wang, Q. Qian, C. Bi, S. Wang, Y. Huang, ACS Appl. Mater. Interfaces 9 (2017) 40969.

[38] W. Xiong, C. Xia, X. Zhao, T. Wang, Y. Jia, Carbon 109 (2016) 737.

[39] P. Giannozzi, S. Baroni, N. Bonini, M. Calandra, R. Car, C. Cavazzoni, D. Ceresoli, G. L. Chiarotti, M. Cococcioni, I. Dabo, A. D. Corso, S. de Gironcoli, S. Fabris, G. Fratesi, R. Gebauer, U. Gerstmann, C. Gougoussis, A. Kokalj, M. Lazzeri, L. Martin-Samos, N. Marzari, F. Mauri, R. Mazzarello, S. Paolini, A. Pasquarello, L. Paulatto, C. Sbraccia, S. Scandolo, G. Sclauzero, A. P. Seitsonen, A. Smogunov, P. Umari, R. M. Wentzcovitch, J. Phys.: Condens. Matter 21 (2009) 395502.

[40] A. Delin, P. Ravindran, O. Eriksson, J. Wills, Int. J. Quantum Chem. 69 (1998) 349.

[41] P. Ravindran, A. Delin, B. Johansson, O. Eriksson, J. M. Wills, Phys. Rev. B 59 (1999) 1776.

[42] S.-D. Guo, Y.-H. Wang, J. Appl. Phys. 121 (2017) 034302.

[43] A. R. H. F. Ettema, R. A. de Groot, C. Haas, T. S. Turner, Phys. Rev. B 46 (1992) 7363.

[44] L. C. Gomes, A. Carvalho, A. H. Castro Neto, Phys. Rev. B 92 (2015) 214103.

[45] A. Walsh, G. W. Watson, Phys. Rev. B 70 (2004) 235114.

[46] G. A. Tritsaris, B. D. Malone, E. Kaxiras, J. Appl. Phys. 113 (2013) 233507.

[47] J. R. Brent, D. J. Lewis, T. Lorenz, E. A. Lewis, N. Savjani, S. J. Haigh, G. Seifert, B. Derby, P. O'Brien, J. Am. Chem. Soc. 137 (2015) 12689.

ACCEPTED MANUSCRIPT

[48] N. Koteeswara Reddy, Y. B. Hahn, M. Devika, H. R. Sumana, K. R. Gunasekhar, J. Appl. Phys. 101 (9) (2007) 093522.

ACCEPTED MANUSCRIPT